Iran J Sci Technol Trans Mech Eng (2018) 42:41–49
https://doi.org/10.1007/s40997-017-0075-3

CrossMark

RESEARCH PAPER

Analysis of Void Growth During Superplastic Deformation of Commercial AL5083 Alloy

M. E. Hosseini[1] · S. J. Hosseinipour[1] · M. B. Jooybari[1]

Received: 24 August 2014 / Accepted: 10 December 2016 / Published online: 3 March 2017

Abstract Superplastic alloys and metals possess the ability to undergo large uniform strains prior to failure. A number of materials are subject to the cavitation during superplastic deformation. Cavitation usually leads to either the undesirable post-forming characteristics or to the premature tensile failure. It is also apparent that the cavities can preexist in the form of cracks and decohered interfaces, which develop during thermo-mechanical processing necessary to produce the superplastic microstructures. Evidently, extensive cavitation imposes significant limitations on their commercial application. The material constitutive equation constants of commercial AL5083 alloy contain strength coefficient, and strain rate sensitivity index is determined by superplastic bulge forming tests for 400, 450, 500, 550 °C. By comparing the results of a deformed sample, good accordance between experimental and FEM results is observed. Using the calculated values for C and m parameters, the effect of material properties such as the cavity growth rate, strain rate sensitivity index, strain hardening exponent and number of intentionally preexisted voids on specimens voids growth subject to the tensile deformation and to the biaxial deformation has been determined numerically. The tensile tests have been simulated by the FEM software ABAQUS v6.9 using commercial aluminum 5083 alloy that presents superplastic properties at temperatures in the range 400–550 °C. The simulations are implemented at 400, 450, 500 and 550 °C. The results of the numerical prediction obtained are in good agreement with the results of the experiments done by some other authors.

Keywords Superplasticity · Cavitation · Voids growth · Aluminum 5083 · Finite element method

1 Introduction

The reason for the spread of superplastic materials is due to their exceptional ductility in particular conditions. Indeed, in some cases tensile elongations above 7000% were achieved, even if, in industrial applications typical values are comprised between 200 and 1000% (Langdon 1995). It is important to note that such values are greater by one or two orders of magnitude compared to those of conventional metallic materials. As regards isothermal superplasticity, which is the one considered in industrial cases, the conditions that must be respected for a metal or a metallic alloy to exhibit superplastic behavior regard both material microstructure and the operating parameters adopted during the forming process. In particular, the material must have a grain size of less than 10 μm, and forming must take place at a temperature that is constant and equal to at least half the absolute melting point, and at a very low strain rate, in the order of 10^{-5} to $10^{-3}s^{-1}$ (Langdon 1995). It is observed that the value of the strain rate sensitivity index (m) has a strong effect on the ductility of superplastic materials. In general, the higher the m value, the greater the elongation to failure (Kim et al. 1996; Carrino et al. 2001, 2003). Shehata et al. (1978) examined the formability of several Al–Mg alloys at temperatures from room temperature to 300 °C over a wide range of strain rates by performing uniaxial and biaxial stretch forming tests. Naka

✉ M. E. Hosseini
emad_hoseiny@yahoo.com

[1] Department of Mechanical Engineering, Babol Noshirvani University of Technology, Babol, Iran

et al. (2001) investigated the effect of forming speed and temperature on the formability of AA5083 alloy sheet by stretch forming tests with a flat head cylindrical punch at various forming speeds and temperatures from room temperature to 300 °C. Hosseinipour (2009) studied the hot deformation behavior of AA5083 with tensile tests at various temperatures and strain rates. The results showed that the formability increased with decreasing speed for any strain paths at high temperature, while at room temperature it was not as sensitive to speed. Hosseinipour (2010) investigated the strain rate sensitivity and cavitation in a commercial 5083 aluminum alloy. The results showed that with increasing temperature the maximum strain rate sensitivity decreases and shifts to the lower strain rates. The failure surface is wide and failure occurs by cavitation. Chung and Cheng (2002) showed that, in some superplastic materials, the fracture mode is dominated by unstable plastic flow. The instability of superplastic deformation was studied by several investigators by analytical approaches. Pearce (1989) showed that in the tensile test the shrinkage rate is inversely proportional to the cross section of the specimen and highly sensitive to the strain rate sensitivity index.

Strain rate control assumes a fundamental role. So that the strain rate sensitivity index, m, attains a maximum value. This condition permits high material formability, m, being directly proportional to the material elongation capability.

This high ductility can be easily exploited to form complex shapes making superplastic forming technology of notable interest for the metal forming industry, particularly for the aerospace applications. This ability to reach large strains is limited by the fact that such materials are susceptible to internal voids formation, which may eventually lead to failure in the specimen. The cavitation process is comprised of three distinct stages, which in most cases occur simultaneously: cavity nucleation, cavity growth and cavity coalescence.

Cavities, which preferentially nucleate at irregularities of the grain boundary, triple point or second-phase particles, grow by either plastic deformation (Hancock 1976; Cocks and Ashby 1980) or diffusion-controlled mechanism (Chokshi and Langdon 1990), or a combination of the two. The cavity coalescence occurs during the last stages of the deformation process by which time a large cavity volume fraction has developed (Pilling and Ridley 1989). The plasticity-controlled cavity growth is described by the following equation (Pilling and Ridley 1989):

$$\frac{\mathrm{d}r}{\mathrm{d}\varepsilon} = \frac{\eta}{3}\left(r - \frac{3\gamma}{2\sigma_e}\right) \tag{1}$$

where r is the cavity radius, ε the strain, γ the surface energy of cavity, σ_e the effective stress and $\eta = d\ln v/d\varepsilon$ is the cavity growth rate factor, where v is the volume of a single cavity. This volumetric growth rate factor, η, described by Cocks and Ashby (1980), Stowell et al. (1984) and Pilling and Ridley (1989), in terms of strain rate sensitivity (m), the applied stress state and stress concentration factor (k_s), is expressed as follows:

$$\eta = \frac{3}{2}\left(\frac{m+1}{m}\right)\sinh\left[2\left(\frac{2-m}{2+m}\right)\left(\frac{k_s}{3} - \frac{p}{\sigma_e}\right)\right]. \tag{2}$$

where P is the imposed pressure, k_s depends on the geometry of deformation and the extent of grain boundary sliding (Cocks and Ashby 1980; Pilling and Ridley 1989) and:

$$\left(\frac{k_s}{3} - \frac{p}{\sigma_e}\right) = \frac{\sigma_m}{\sigma_e}. \tag{3}$$

where σ_m is the mean stress. Stowell (1980) by assuming a certain level of preexisting voids within the material gives:

$$C_v = C_0 \exp(\eta\varepsilon) \tag{4}$$

where C_v is the cavity volume fraction and C_0 the initial volume fraction of cavities. To reduce the level of cavitation for a given strain, it is necessary to reduce the magnitude of η, the cavity growth parameter, which depends on m and the ratio σ_m/σ_e (Eqs. 2 and 3). Diffusional cavity growth occurs by the stress-directed diffusion of vacancies in the cavities, usually along grain boundaries. This model predicts the following growth rate:

$$\frac{\mathrm{d}r}{\mathrm{d}\varepsilon} = \frac{\Omega\delta D_{\mathrm{gb}}}{5kTr^2}\frac{\sigma - 2\gamma}{r} \tag{5}$$

where r is the cavity radius, $\mathrm{d}r/\mathrm{d}\varepsilon$ the cavity growth rate per unit strain, Ω the atomic volume, δ the grain boundary width, D_{gb} the coefficient for grain boundary diffusion, k the Boltzmann's constant, T the absolute temperature and γ the surface energy (Chokshi 1986).

In the early stages, the voids shape of deformation is elliptical, the hole increases in length along the tensile axis but it decreases along the perpendicular direction to the tensile axis (transverse contraction), subsequently, the hole grows both along and perpendicular to the tensile axis (transverse growth), and finally, a crack nucleates on either side of the hole and it propagates to cause failure (crack propagation) (Chokshi and Langdon 1996). A special aspect of the growth problem is the effect of voids interaction on the macroscopic mechanical behavior (ductility and flow stress) of the investigated material. The numerical and experimental studies have revealed that the parameters affecting voids growth in the superplastic deformation are the strain rate sensitivity (m), the voids size and the number of the existing voids (Khraishi et al. 2001). Carrino et al. (2004) investigated the effects of some material properties such as void growth rate, void numbers, strain rate

sensitivity index and strain hardening exponent on void growth and material ductility of fine-grained Pb–Sn alloy that presents superplastic behavior at room temperature by experimental procedure and FEM at tensile deformation and biaxial deformation. They stated that increasing the void numbers and decreasing of m and n leads to decrease in void growth and increase in material ductility. Lin et al. (2005) collected contents for different damage mechanisms of metallic materials at various deformation conditions of high-temperature creep, cold metal forming, superplastic forming and hot metal forming. They reviewed and discussed the ruling equations and damage calibration techniques for these deformation conditions. Mulholland et al. (2006) conducted a set of parametric experiments of simple superplastic tensile test on a pre-machined superplastic eutectic tin lead alloy with one or more holes. Their results indicated an increase in ductility by increasing hole numbers up to 10 holes, and decrease in ductility by increasing the hole numbers more than 10 holes. Hosokawa et al. (2013) experimentally investigated the influences of material work-hardening behavior of some materials on fracture mechanism and void growth and coalescence, using in situ X-ray computed tomography (XCT) along with tensile test on specimens including artificial void array. Also, they used Thomason, Pardeon and Hutchinson models for void coalescence.

In this paper, at first the material constitutive equation constants including strength coefficient and strain rate sensitivity index are calculated by gas blow forming bulge tests at different superplastic hot temperatures 400, 450, 500, 550 °C for commercial AL5083 alloy. Then, by using these values, a comparison of a sample dome heights between experimental and FEM results has been made. A good agreement between two sets of results has been obtained. Similar to work done by Carrino et al. (2004), the effect of material parameters (m and n), η and number of voids on the voids growth is analyzed with finite element method. In the case of uniaxial tension 1, 3 and 5, preexisted voids have been considered and an only void in the case of biaxial tension has been considered. Finally, the true stress–strain curves have been investigated for mentioned hot temperatures.

2 Experimental Material and Procedures

The simple tensile test samples are clamped at the bottom side and at the top side are stretched with a velocity in accordance with the strain rate defined. This velocity can be calculated using Eq. (6):

$$v = \dot{\varepsilon}.L \tag{6}$$

where L is the instantaneous length of the sample and $\dot{\varepsilon}$ is the constant strain rate. A power law form of the constitutive relationship is assumed:

$$\bar{\sigma} = C\dot{\bar{\varepsilon}}^{m} \tag{7}$$

where $\bar{\sigma}$ is the effective stress, $\dot{\bar{\varepsilon}}$ is the effective strain rate, C is a constant, and m is the strain rate sensitivity index.

The material characteristics in the hot condition were determined by bulge tests with the gas blow forming process at various temperatures and pressures using the following equation (Giuliano and Franchitti 2008; Sorgente and Scintilla 2010):

$$m = \frac{\ln(P_1/P_2)}{\ln(t_2/t_1)} \tag{8}$$

where t_1 and t_2 are the forming times necessary to obtain the same dome height at constant pressures of p_1 and p_2, respectively. The dome height during the bulge test was measured by an ultrasonic telemetry sensor.

The equivalent stress, strain and strain rate in the dome apex were calculated using the following equations (Liu et al. 2008; Koç and Billur 2011):

$$\bar{\sigma} = \frac{pr}{2s} \tag{9}$$

where:

$$r = \frac{h^2 + (d/2)^2}{2h} \tag{10}$$

and

$$\bar{\varepsilon} = ln\frac{s}{s_0} \tag{11}$$

and

$$\dot{\bar{\varepsilon}} = \frac{\bar{\varepsilon}}{t} \tag{12}$$

where r is the dome radius, s is the final thickness of the dome apex, s_0 is the initial thickness of the blank, h is the dome height, d is the die diameter, and t is the forming time.

In order to validate the finite element simulations, a comparison between experimental test and FEM simulation has been made. The experiments were conducted using a commercial AL5083 alloy, which is known to exhibit superplastic properties at temperatures 400–550 °C. The bulge tests were carried out using a set of equipment (Fig. 1) at constant pressures 0.2 MPa and 0.3 MPa to establish the constitutive equation of the material. If we assume these two pressures as p_1 and p_2, for a constant value of bulge height, the times to reach this bulge height are recorded as t_1 and t_2. The strain rate sensitivity, m, is

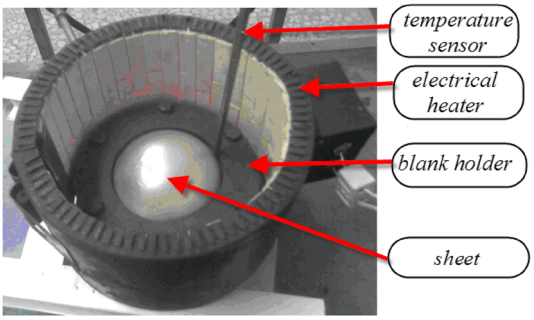

Fig. 1 Equipment used to carry out the superplastic forming

calculated by Eq. (8) (Giuliano and Franchitti 2008). The material constitutive equation is assumed as Eq. (7).

These tests have been implemented for temperatures 400, 450, 500 and 550 °C, and strain rate sensitivity and strength coefficient were calculated (Table 1).

Figure 2 shows the comparison between two samples bulged at constant pressure 2 bar and at temperature 500 °C, FEM is simulated on top and experimental sample at the bottom.

Figure 3 shows the comparison of dome height of sample during sheet forming, between experimental and simulation results. The figure shows the good agreement between experimental and numerical simulation results.

3 Numerical Analysis

In this work, the numerical studies of the growth of the voids and the parameter that affect it were carried out. The finite element calculations were performed using the *ABAQUS* v6.9 software package. Initially, each finite element model was used to simulate a thin plate (plane stress conditions) with preexisting holes subjected to a constant pressure. Figure 4 shows the meshes of tensile specimens with three different hole configurations: a central hole, three equally spaced holes and five equally spaced holes. The 2D modeling, using four-noded continuum elements, was examined. The initial holes have the form of a circle and a radius that is equal to 640 μm.

Due to the symmetry of the loading and the geometry, only the first quadrant was used in the calculations. The single-hole mesh had 235 quadrilateral elements with 277 nodes. The three-hole mesh had 505 elements with 568 nodes, and finally, the five-hole mesh had 825 elements with

Table 1 Constitutive equation constants of commercial Al5083 alloy

Temperature (°C)	400	450	500	550
m	0.25	0.32	0.35	0.34
C (MPa)	138.9	136	116.9	68

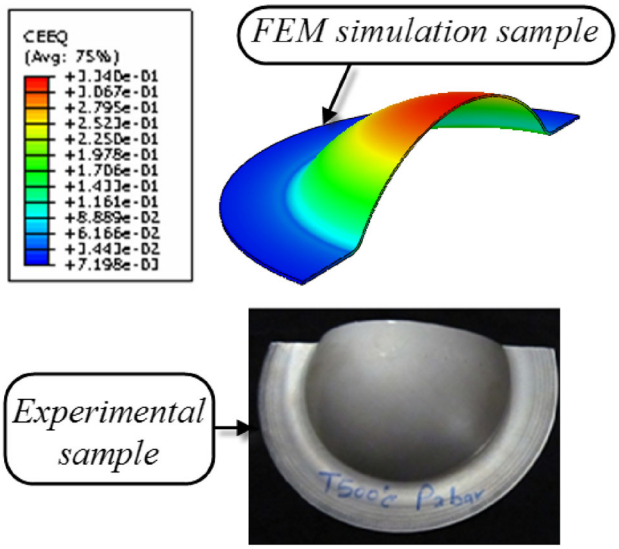

Fig. 2 Comparison between simulated sample and experimental one

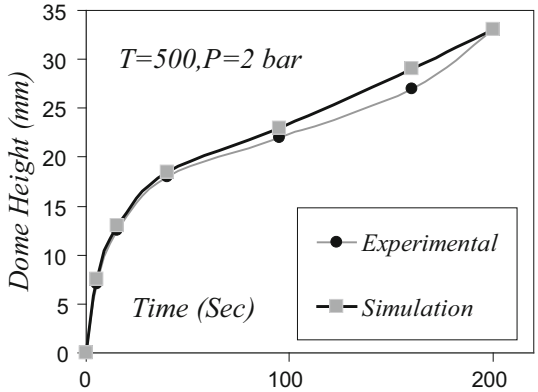

Fig. 3 Comparison of sample dome height between experimental and numerical simulation

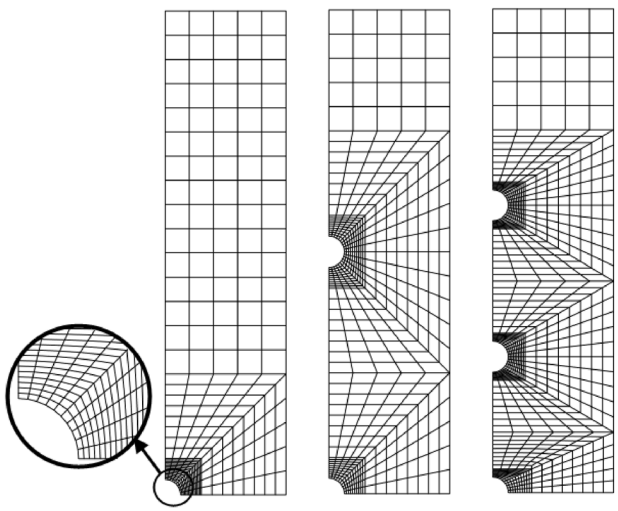

Fig. 4 Typical finite element meshes with a central hole, three holes and five holes

919 nodes. The bottom and the left edges of the sample were clamped by symmetry boundary conditions. At the top edge of the sample, constant pressure was applied.

In the case of biaxial deformation, a single hole was realized in the center of a sheet with a width of 150 mm and, due to the symmetry, the first quadrant was examined. The mesh had 105 quadrilateral elements for axisymmetric applications with 212 nodes. The FEM mesh and the die are shown in Fig. 5. The nodes along the die entry radius are fixed in the y-direction except for one, which is fixed in the x-direction in order to simulate the presence of a blank-holder. The element type CPS4R was used in the FEM simulations. This is a 4-node bilinear plane stress quadrilateral, reduced integration, hourglass control element. The element shape is quad, and the technique of meshing is structured.

A constitutive equation, which defined the relationship between the flow stress, σ, the strain, ε and the strain rate, $\dot{\varepsilon}$, was employed as:

$$\sigma = k\varepsilon^n \dot{\varepsilon}^m. \tag{13}$$

where k is the strength coefficient, m the strain rate sensitivity index and n the strain hardening index.

The critical variables in the present model are the material parameters (m and n) and the strain. The m value has been varied between 0.25 and 0.35 (0.25, 0.32, 0.342 and 0.35), and n had the following values: 0, 0.0334, 0.0667 and 0.1. The voids growth was valued, considering the parameters: normalized minor radius $r_{\min}/r_0$, normalized major radius $r_{\max}/r_0$, normalized area A/A_0 and the void growth rate η, depending on elongation(%), m and n. If we assume $C_v/C_0 = A/A_0$, according to Eq. (4), it can be shown that:

$$\eta = \ln\left(\frac{A/A_0}{\varepsilon}\right). \tag{14}$$

4 Results and Discussions

Figures 6 and 7 show the material constants at elevated temperatures and various strain rates which were obtained by bulge tests using the gas blow forming process. The material constants were calculated at different dome heights, and the mean values were reported. As can be seen, with increasing temperature the m value increased, and the maximum m value was obtained at 500 °C, but the C constant decreased with increasing temperature.

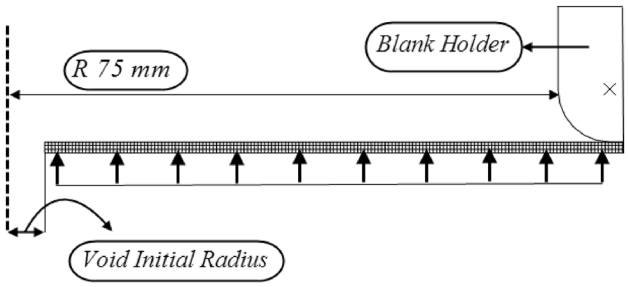

Fig. 5 FEM mesh and die illustration

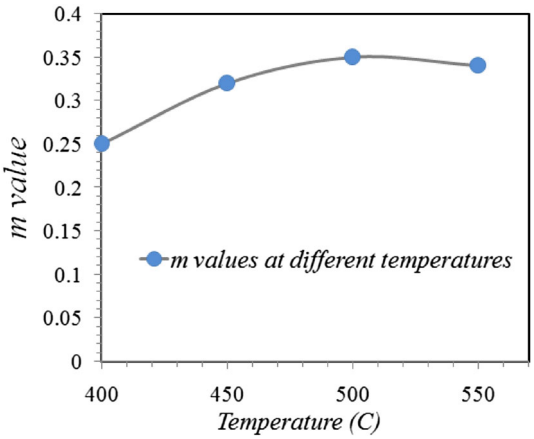

Fig. 6 The m value at various temperatures

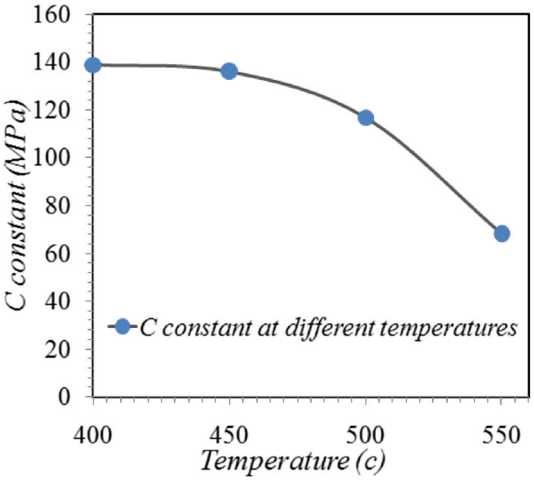

Fig. 7 The C constant at various temperatures

As shown in Fig. 8, the results of numerical analysis indicate that, in the case of a single hole preexisted, the growth of the voids increases with increasing sample elongation and depends on m and n parameters. The void growth (measured by A/A_0) is relatively small for high m values, fixed $n = 0$, and always becomes important for small m values ($m = 0.25$).

Analogously, as shown in Fig. 9, fixed $m = 0.25$, the void growth evolves with decreased n values as also reported in other works (Khraishi et al. 2001; Carrino et al. 2003). By increasing the values of true strain, the void growth rate parameter, η, at first decreases and then begins to increase. The variation tilt of void growth rate, at bigger n values is low, but at low n values the η parameter varies with higher intensity. The η values decrease by increase in

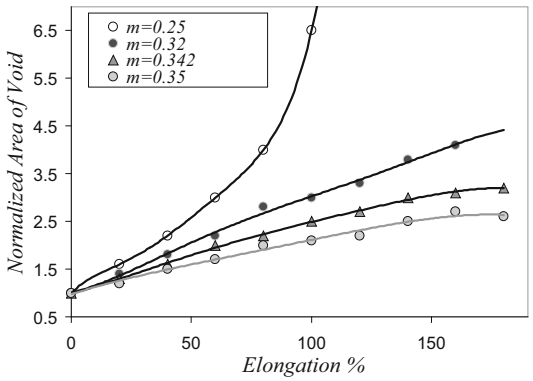

Fig. 8 The effect of strain rate sensitivity on the single void growth ($n = 0$)

the n value. For high m values ($m > 0.32$), the influence of the strain hardening becomes unimportant.

The effect of multiple holes was analyzed, considering three and five holes aligned along the major axis. The tensile test output is represented by the variation of normalized minor and major radii of voids with sample elongation, normalized void area with elongation and void growth rate parameter, η, with true strain. For brevity, only the curves relative to five holes, fixed $m = 0.25$, are reported in Fig. 9.

The performance of the multiple-hole curves is the same as the single-hole curves with varying m and n parameters, but by increasing the number of holes, along the major axis the effect of increasing the metal ductility is observed. This

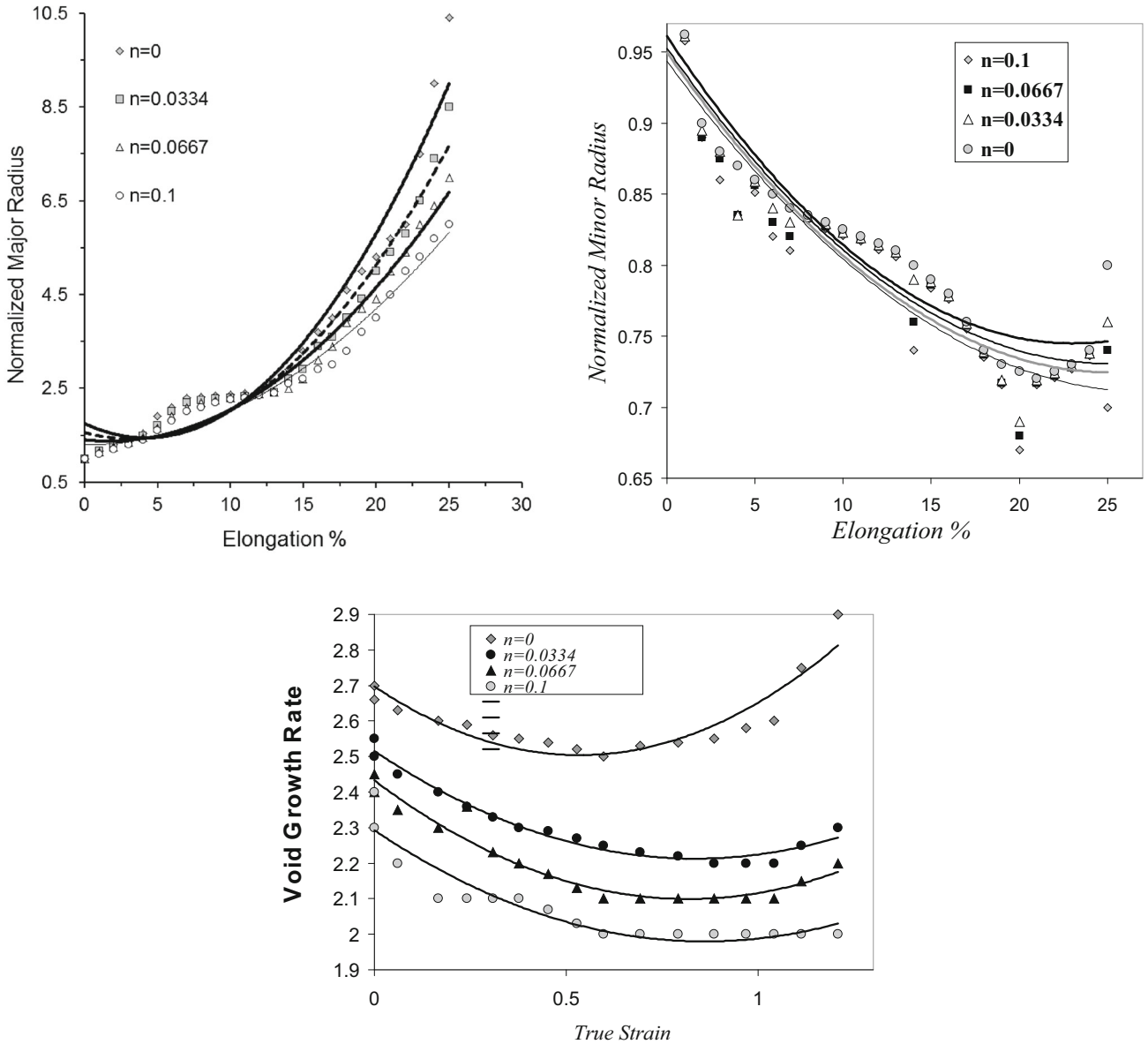

Fig. 9 The effects of strain hardening index on the growth of the five voids $m = 0.25$)

occurs when the extent of necking is reduced and its onset delayed through dispersing the plastic deformation at the different hole sites and also reducing the stress concentration. Besides, the elongation of the major radius is restricted by neighboring holes and cannot achieve values attained by a single-hole specimen for the same given strain. Figure 10 shows a decrease in a major radius and a neck-in, in accordance with the holes, by increasing the number of holes. Those results are in good qualitative agreement with the results of Khraishi et al. (2001).

The effect of multiaxial modes of deformation was investigated, varying m and n parameters and valuing the single void growth (measured by normalized area) depending on true strain (measured by the height of free forming specimens). In the case of the biaxial deformation, the form of the hole does not change during the superplastic forming. Fixing n, the normalized area increases by decreasing the m parameter, which is obviously shown in Fig. 11 which shows that at high m values ($m \geq 0.32$), the void growth procedure happens gradually, but at $m = 0.25$ which refers to the temperature of 400 °C, by increasing the true strain value, void growth occurs with high tilt and intensity. The results of numerical analysis are shown in Fig. 11.

Figure 12 shows the deformed mesh, fixed $h = 17$ mm and $n = 0$, for the m values of 0.25 and 0.35, and the major void growth is observed at $m = 0.25$. Besides, the numerical results indicate that the radius of the hole is increased by increasing the height (true strain) of the specimen. High ductility increasing can be seen by the increase in m value.

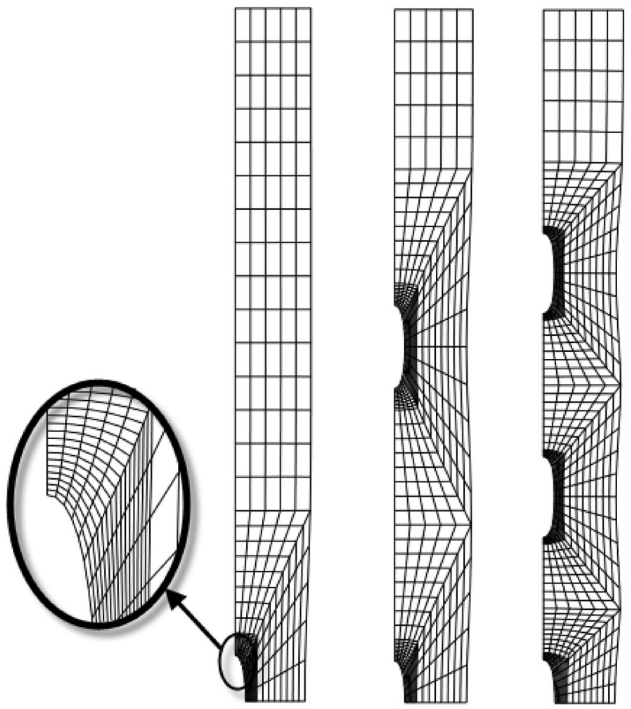

Fig. 10 Typical deformed voids shapes at elongation = 104.2%, $m = 0.25$ and $n = 0$

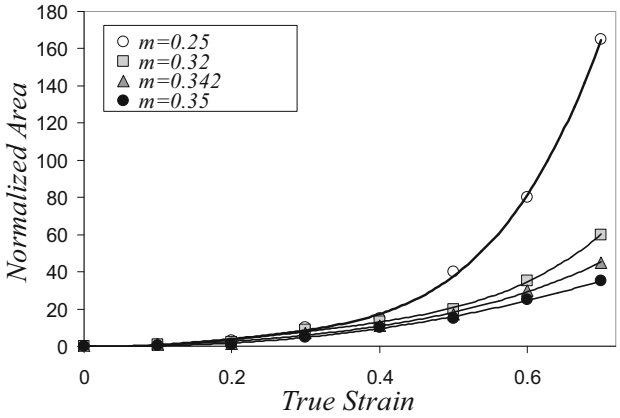

Fig. 11 The effects of strain rate sensitivity on the single void growth ($n = 0$) in the biaxial deformation

In Fig. 13, the evolution of the void growth is reported in four different levels of deformation. Comparing uniaxial and biaxial deformation (Fig. 14) in the case of a single void, the void growth (measured by the normalized area) is more important for the biaxial deformation by increasing the true strain.

Figure 15 shows the parameter void growth rate, η, for different m values. For all m values, the void growth parameter η sharply increased at low strains, but after reaching a maximum value, η began to decrease by plastic deformation evolvement. η values rose with decrease in m parameter.

Figure 16 shows the evolution of void growth in simple tensile test. At first, the void growth velocity is low, but suddenly begins to grow fast.

The stress–strain curves at various temperatures are illustrated in Fig. 17. It appears that at lower strain after high initial stress, flow stress begins to gradually fall with strain, and at higher strain, the flow stress reaches a steady-state stress. This kind of strain softening is normally observed when the material exhibits continuous recrystallization during hot deformation where the deformed grains are replaced by strain-free grain.

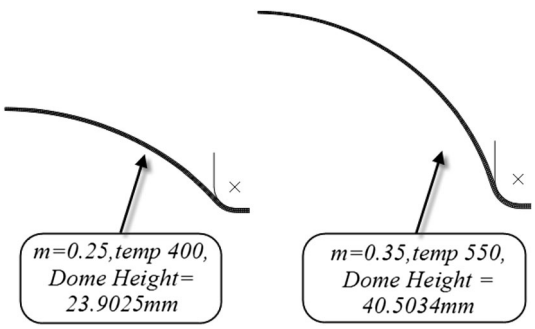

Fig. 12 Typical voids growth, $n = 0$, for $m = 0.25$ and $m = 0.35$

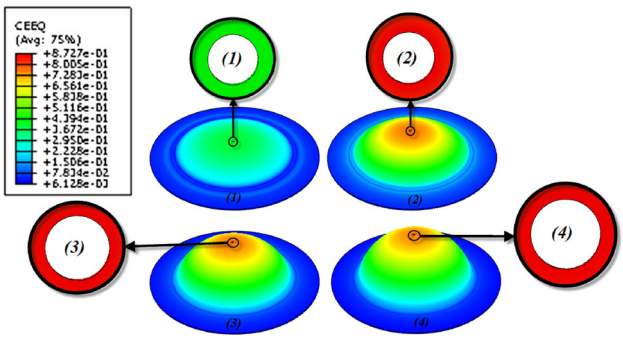

Fig. 13 Evolution of void growth in four different levels of deformation for $m = 0.35$, $n = 0$

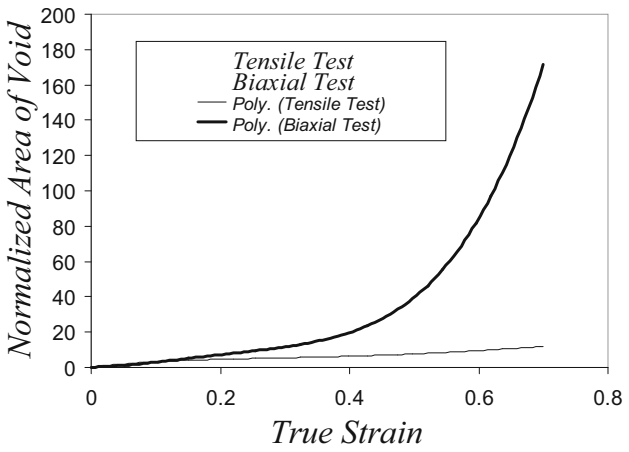

Fig. 14 The effects of the tension state on the void growth

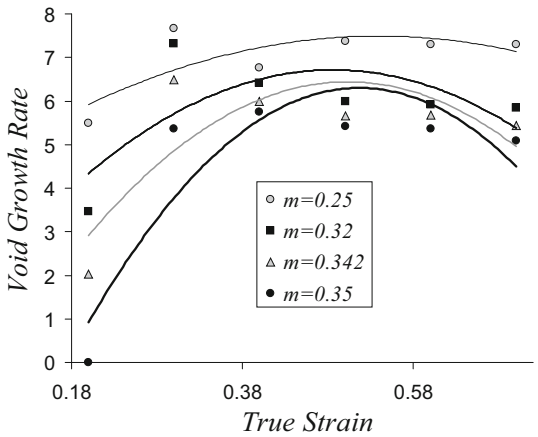

Fig. 15 Void growth rate parameter for different m

5 Conclusion

The material constitutive equation constants, strength coefficient (c) and strain rate sensitivity index (m), were obtained using gas blow forming bulge tests at different superplastic hot temperatures 400, 450, 500, 550 °C for commercial AL5083 alloy. Using these values and by comparing sample dome heights between experimental and FEM results, good agreement between these two sets of results was observed. Finite element software ABAQUS v6.9 was used to investigate the parameters affecting the growth of the preexisted voids in the commercial AL5083 alloy by the numerical tests in two stress states, uniaxial superplastic tensile test and biaxial superplastic bulge test. The stress–strain curves at various temperatures were illustrated and discussed. The m values increased by temperature evolving at 500 °C; the maximum m values were obtained, but the strength coefficient decreased by increase in temperature. The voids growth increased with elongation increasing. The void growth is independent from the strength coefficient value and the applied strain rate, but it is dependent on the strain rate sensitivity and the strain hardening index. It is also small for high m values and important for small m values. The void growth rate

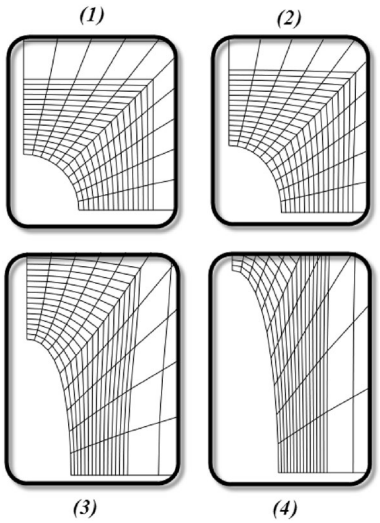

Fig. 16 Void growth evolution in simple tensile test

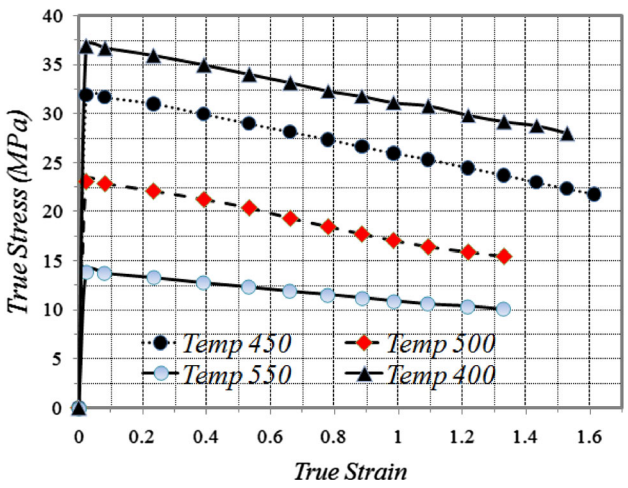

Fig. 17 The stress–strain curves at various temperatures

parameter, η, decreases with an increase in n. The effect of strain hardening is unimportant for high m values. The multiple holes aligned along the major tensile axis had the effect of decreasing the growth of the voids and, therefore, the ductility of the materials. The normalized area of voids increased by decreasing the m parameter. Generally by increasing m value, high ductility increase was observed. The biaxial deformation involved an increase in the void growth, compared with the uniaxial deformation, by increasing the true strain. Besides, in the biaxial deformation, the void growth increases by decreasing the m and n values. The void growth rate parameter values, η, shifted upward by decrease in m parameter. For all stress–strain curves at different temperatures, at lower strain after high initial stress, the stress values started to fall gradually with increase in strains, and at higher strains, the stress value achieved a steady-state stress.

Acknowledgements The authors would like to appreciate the office of the Vice President for Research of Babol Noshirvani University of Technology for its financial support.

References

Carrino L, Giuliano G, Palmieri C (2001) Analysis of superplastic bulge forming by the finite element method. J Mater Process Technol 16:237–241

Carrino L, Giuliano G, Polini W (2003a) A method to characterise superplastic materials in comparison with alternative methods. J Mater Process Technol 138:417–422

Carrino L, Giuliano G, Napolitano G (2003b) A study of premachined hole growth in superplastic materials. Mater Des 24:137–142

Carrino L, Giuliano G, Ucciardello N (2004) Analysis of void growth in superplastic materials. J Mater Process Technol 155–156:1273–1279

Chokshi AH (1986) The development of cavity growth maps for superplastic materials. Mater Sci 21:2073–2082

Chokshi AH, Langdon TG (1990) Nucleation and growth of cavities in a superplastic quasi-single phase copper alloy. Acta Metall 38:867–877

Chokshi AH, Langdon TG (1996) A model study of cavity growth in superplasticity using single premachined holes. Metall Mater Trans 27A:2532–2539

Chung LC, Cheng JH (2002) Fracture criterion and forming pressure design for superplastic bulging. Mater Sci Eng A 33:146–151

Cocks ACF, Ashby MF (1980) Intergranular fracture during power-law creep under multiaxial stresses. Met Sci 14:395–402

Giuliano G, Franchitti S (2008) The determination of material parameters from superplastic free-bulging tests at constant pressure. Int J Mach Tools Manuf 48:1519–1522

Hancock JW (1976) Creep cavitation without a vacancy flux. Met Sci 10:319–326

Hosokawa A, Wilkinson DS, Kang J, Kobayashi M, Toda H (2013) Void growth and coalescence in model materials investigated by high-resolution X-ray microtomography. Int J Fract 181(1):51–66

Hosseinipour SJ (2009) An investigation into hot deformation of aluminum alloy 5083. Mater Des 30:319–322

Hosseinipour SJ (2010) Strain rate sensitivity and cavitation in superplastic deformation of a commercial Al-5083 alloy. Adv Mater Res 83–86:400–406

Khraishi TA, Khaleel MA, Zbib HM (2001) A parametric-experimental study of void growth in superplastic deformation. Int J Plast 17:297–315

Kim YH, Hong SS, Lee JS, Wagoner RH (1996) Analysis of superplastic forming processes using a finite-element method. J Mater Process Technol 62:90–99

Koç M, Billur E (2011) An experimental study on the comparative assessment of hydraulic bulge test analysis methods. Mater Des 32:272–281

Langdon TG (1995) Superplasticity: 60 years after Pearson. Bourne Press, Bournemouth, p 9

Lin J, Liu Y, Dean TA (2005) A review on damage mechanisms, models and calibration methods under various deformation conditions. Int J Damage Mech 14(4):299–319

Liu J, Chen Z, Yan H (2008) Many-stage gas bulging forming of sheet magnesium alloy AZ31. Met Sci Heat Treat 50:110–114

Mulholland M, Khraishi T, Shen YL, Horstemeyer M (2006) Void growth and interaction experiments: implications to the optimal straining rate in superplastic forming. Int J Plast 22:1728–1744

Naka T, Torikai G, Hino R (2001) The effect of temperature and forming speed on the forming limit diagram for type 5083 aluminum-magnesium alloy sheet. J Mater Process Technol 113:648–653

Pearce R (1989) Superplasticity: an overview. Ashford Press, Curdridge, Southampton

Pilling J, Ridley N (1989) Superplasticity in crystalline solids. The Institute of Metals, London

Shehata F, Painter MJ, Pearce R (1978) Warm forming of aluminum/magnesium alloy sheet. J Mech Work Technol 2:279–290

Sorgente D, Scintilla LD (2010) Blow forming of AZ31 magnesium alloy at elevated temperatures. Int J Mater Form 3:13–19

Stowell MJ (1980) Metal Sci 14:267–272

Stowell MJ, Livesey DW, Ridley N (1984) Cavity coalescence in superplastic deformation. Acta Metall 32:35–42